Lattice QCD at finite isospin density at zero and finite temperature

J. B. Kogut
Department of Physics, University of Illinois, 1110 West Green Street, Urbana, Illinois 61801-3080

D. K. Sinclair
HEP Division, Argonne National Laboratory, 9700 South Cass Avenue, Argonne, Illinois 60439

(Received 23 April 2002; published 22 August 2002)

We simulate lattice QCD with dynamical u and d quarks at finite chemical potential, μ_I, for the third component of isospin (I_3) at both zero and at finite temperature. At zero temperature there is some μ_I, μ_c say, above which I_3 and parity are spontaneously broken by a charged pion condensate. This is in qualitative agreement with the prediction of effective (chiral) Lagrangians which also predict $\mu_c = m_\pi$. This transition appears to be second order, with scaling properties consistent with the mean-field predictions of such effective Lagrangian models. We have also studied the restoration of I_3 symmetry at high temperature for $\mu_I > \mu_c$. For μ_I sufficiently large, this finite temperature phase transition is very abrupt, suggesting that it is first order. As μ_I is decreased it appears to become second order connecting continuously with the zero temperature transition.

DOI: 10.1103/PhysRevD.66.034505 PACS number(s): 11.15.Ha, 12.38.Gc

I. INTRODUCTION

Neutron stars are made of dense cold nuclear matter—hadronic matter at high baryon-number density and low temperature. Large nuclei can be considered as droplets of nuclear matter. The relativistic heavy-ion collisions now being observed at the BNL Relativistic Heavy Ion Collider (RHIC) and the CERN heavy-ion program can produce hadronic matter at high temperature and finite baryon-number density. Nuclear matter also has a finite (negative) isospin (I_3) density due to Coulomb interactions, and it has been suggested that at very high densities it would have a finite strangeness density. Hence it is of interest to study QCD at finite quark/baryon-number density, finite isospin density and finite strangeness density at both zero and finite temperature.

Finite density is customarily studied through the introduction of a chemical potential for the charge of interest in the action. Introducing a finite chemical potential for quark number leads to a complex fermion determinant with a real part of indefinite sign, which precludes the use of standard simulation methods which rely on importance sampling. Methods have been developed recently for simulating the high temperature, low quark-number chemical potential regime of QCD [1]. However, as yet there is no method for studying the low temperature, high chemical potential phases of QCD. If we include a finite chemical potential, μ_I, for I_3 in the absence of any quark-number chemical potential, the fermion determinant remains non-negative, and simulations are possible. Such simulations can determine the QCD phase structure on one surface in the phase diagram for nuclear matter. One can hope that this will identify phases which will persist to finite baryon or quark-number density, and determine their properties.

We have performed simulations of lattice QCD with 2 flavors of light staggered quarks at finite μ_I for both zero and finite temperatures. Preliminary results of these simulations were reported in Ref. [2]. We included a small explicit I_3-breaking interaction needed to observe spontaneous symmetry breaking on a finite lattice. In addition to allowing us to observe spontaneous breaking of I_3 (and parity), this term renders the fermion determinant strictly positive. Our zero temperature simulations were performed on an 8^4 lattice at an intermediate value of the coupling constant. In the limit that our symmetry-breaking parameter vanishes, there is some $\mu_I = \mu_c$ above which I_3 and parity are broken spontaneously by a charged pion condensate. This is in accord with the predictions of Son and Stephanov using effective (chiral) Lagrangians [3]. We observe critical scaling consistent with the mean-field predictions of these effective (chiral) Lagrangians. In drawing these conclusions, it is important to use equations of state of the forms predicted by such effective Lagrangians. Since we draw these conclusions from a single lattice size, they should not be considered definitive. These results are similar to those obtained in studies of the quenched version of this theory [4]. They are also similar to what is observed for 2-color QCD at finite chemical potential μ for quark-number [5–8]. This is not surprising since the effective Lagrangian analysis of 2-color QCD at finite μ [9] is similar to that for QCD at finite μ_I.

Our finite temperature simulations were performed on $8^3 \times 4$ lattices. At sufficiently high temperature and $\mu_I > \mu_c$, we observe the evaporation of the symmetry-breaking pion condensate. For μ_I sufficiently large, this transition is very abrupt, which suggests that it is first order. As $\mu_I \to \mu_c$ this transition softens and appears to become second order. Such a transition from first to second order should occur at a tricritical point. Again these results are similar to what we observed for 2-color QCD at finite quark-number chemical potential [8,10].

Section II gives details of the actions and their symmetries. In Sec. III we present our zero temperature results and scaling analyses. The finite temperature results are presented in Sec. IV. Discussions, conclusions and an outline of planned extensions are given in Sec. V.

II. LATTICE ACTION AND SYMMETRIES

The staggered fermion part of the action for lattice QCD with degenerate u and d quarks at a finite chemical potential μ_I for isospin (I_3) is

$$S_f = \sum_{sites} \bar{\chi}[\not{D}(\tau_3\mu_I) + m]\chi \tag{1}$$

where $\not{D}(\mu)$ is the standard staggered $\not{D}$ with links in the $+t$ direction multiplied by $e^{(1/2)\mu}$ and those in the $-t$ direction multiplied by $e^{-(1/2)\mu}$ [4]. When $\mu_I = m = 0$, this action has a global $U(2)\times U(2)$ flavor symmetry under which

$$\chi \to \exp[i(\theta + \epsilon\phi).\tau]\chi$$
$$\bar{\chi} \to \bar{\chi}\exp[-i(\theta - \epsilon\phi).\tau] \tag{2}$$

where $\tau = (1, \vec{\tau})$, θ and ϕ are site-independent 4-component "vectors," and $\epsilon = \epsilon(x) = (-1)^{x+y+z+t}$. Spontaneous symmetry breaking can occur in any direction in this space. If we keep $\mu_I = 0$ and allow $m \neq 0$, the symmetry is broken down to $U(2)_V$. On the other hand, if we keep $m = 0$ and allow $\mu_I \neq 0$, the symmetry is broken down to $U(1)\times U(1)\times U(1)\times U(1)$ generated by 1, τ_3, ϵ and $\epsilon\tau_3$. Finally in the general case where neither μ_I nor m vanishes, the symmetry is reduced to $U(1)_V \times U(1)_V$ associated with 1 and τ_3.

In order to predict potential symmetry breaking patterns we make several simple modifications of the arguments of Son and Stephanov [3] to apply them to the staggered lattice action. The generic quark bilinear which creates a meson has the form

$$M = \bar{\chi}\Gamma\chi. \tag{3}$$

The propagator for such a meson obeys the inequality

$$|\langle M(x)M^\dagger(0)\rangle| \leq \text{const} \times \langle S(x,0)S^\dagger(x,0)\rangle. \tag{4}$$

Thus, meson operators M whose propagators are proportional to $\langle S(x,0)S^\dagger(x,0)\rangle$ are potential Goldstone bosons. Now we note that our Dirac operator obeys

$$\tau_{1,2}\epsilon[\not{D}(\tau_3\mu_I) + m]\epsilon\tau_{1,2} = [\not{D}(\tau_3\mu_I) + m]^\dagger, \tag{5}$$

so $i\bar{\chi}\epsilon\tau_{1,2}\chi$ are Goldstone candidates. These are linear combinations of π^+ and π^- creation operators which means that if spontaneous breaking of the remnant flavor symmetry should occur, one linear combination of $\pi^\pm$ will become a Goldstone boson while the orthogonal linear combination will develop a vacuum expectation value—a charged pion condensate. We note, in passing, that in the limit of massless quarks

$$\tau_{1,2}\not{D}(\tau_3\mu_I)\tau_{1,2} = -\not{D}(\tau_3\mu_I)^\dagger, \tag{6}$$

and we have 2 additional Goldstone boson candidates, $\bar{\chi}\tau_{1,2}\chi$, and if spontaneous symmetry breaking does occur we will have 2 Goldstone bosons rather than 1.

Since, in order to observe spontaneous symmetry breaking on a finite lattice, one needs to add a small explicit symmetry breaking term in the direction defined by the condensate, we choose to work with the fermion action

$$S_f = \sum_{sites} [\bar{\chi}[\not{D}(\tau_3\mu_I) + m]\chi + i\lambda\epsilon\bar{\chi}\tau_2\chi] \tag{7}$$

where the term proportional to the (small) parameter λ serves this purpose. The Dirac operator now has the determinant

$$\det[\not{D}(\tau_3\mu_I) + m + i\lambda\epsilon\tau_2] = \det[\mathcal{A}^\dagger\mathcal{A} + \lambda^2] \tag{8}$$

where we have defined

$$\mathcal{A} \equiv \not{D}(\mu_I) + m. \tag{9}$$

(Note that this is a 1×1 matrix in the flavor space on which the τ's act.) We see that adding this symmetry breaking term has the effect of rendering the determinant strictly positive, which enables us to use the hybrid molecular-dynamics (HMD) algorithm to simulate this theory. Note that this theory has 8 continuum flavors. We use the HMD method to take the required fourth root of the determinant reducing this to 2 continuum flavors. For the purpose of simulation, it is convenient to multiply the Dirac operator on the left by the matrix diag$(1,-\epsilon)$ and on the right by the matrix diag$(1,\epsilon)$. The transformed matrix $\tilde{\mathcal{M}}$ has the same determinant as the original Dirac operator, and $\tilde{\mathcal{M}}^\dagger\tilde{\mathcal{M}}$ is block diagonal, with the upper and lower blocks having the same determinant. This means that we use "noisy" fermions and generate Gaussian noise for both upper and lower components of $\tilde{\mathcal{M}}\dot{\chi}$, but only keep the upper components of $\dot{\chi}$ after the inversion. Thus we still have only 8 flavors in the quadratic formulation. This is completely analogous to the odd-even lattice separation which prevents further species doubling in staggered lattice QCD at zero chemical potential.

Quantities we measure include the chiral condensate

$$\langle\bar{\psi}\psi\rangle \Leftrightarrow \langle\bar{\chi}\chi\rangle, \tag{10}$$

the charged pion condensate

$$i\langle\bar{\psi}\gamma_5\tau_2\psi\rangle \Leftrightarrow i\langle\bar{\chi}\epsilon\tau_2\chi\rangle \tag{11}$$

and the isospin density

$$j_0^3 = \frac{1}{V}\left\langle\frac{\partial S_f}{\partial\mu_I}\right\rangle. \tag{12}$$

Here we have included both the lattice and continuum versions of the condensates. To get this simple continuum form for the charged pion condensate requires absorbing a factor of ξ_5 (the flavor analogue of γ_5) into the definition of the d-quark field.

III. LATTICE SIMULATIONS AT ZERO TEMPERATURE

We have simulated $N_f = 2$ lattice QCD at finite μ_I on an 8^4 lattice at an intermediate coupling $\beta = 6/g^2 = 5.2$. This β was chosen since it represents an approximate lower bound

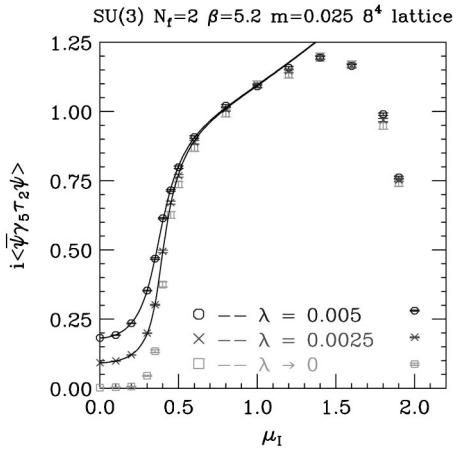

FIG. 1. Charged pion condensate as a function of μ_I for $\lambda = 0.0025$, $\lambda = 0.005$, and $\lambda \to 0$. The curves are fits of the finite λ measurements to the scaling forms defined in the text.

to estimates of the finite temperature transition value for $N_t = 4$ in the chiral limit. This was used to keep finite volume effects at acceptable levels. We performed simulations at 2 different quark masses ($m = 0.025$ and $m = 0.05$) to see that varying the mass did not affect the qualitative behavior of the theory and that we understood the effects of changing the quark mass.

At $m = 0.025$, we performed runs, each of 2000 molecular-dynamics time units in length, at 17 different μ_I values ($0 \leqslant \mu_I \leqslant 2$) for each of $\lambda = 0.0025$ and $\lambda = 0.005$. Using two λ values, both chosen to be much less than m, enabled us to extrapolate to the $\lambda = 0$ limit, which is our ultimate interest. (We also ran at $\mu_I = 3.0$, $\lambda = 0.005$ to check saturation.)

The charged pion condensates $i\langle \bar{\psi}\gamma_5\tau_2\psi\rangle$ from these simulations are presented in Fig. 1 as functions of μ_I, along with a linear extrapolation to $\lambda = 0$. This extrapolation strongly suggests that the $\lambda \to 0$ condensate vanishes for $\mu_I < \mu_c \sim 0.3$–0.45, above which it is finite. This would indicate a phase transition to a phase in which I_3 symmetry is broken spontaneously by a charged pion condensate, with an associated Goldstone mode.

This behavior is predicted by the effective (chiral) Lagrangian analyses of Son and Stephanov, which also predict that the transition should be second order with mean-field exponents [3]. We fit our extrapolated ''data'' to the critical scaling form

$$i\langle \bar{\psi}\gamma_5\tau_2\psi\rangle = \text{const} \times (\mu_I - \mu_c)^{\beta_m} \tag{13}$$

for $\mu_I > \mu_c$ close to the transition. Fitting to this form over the range $0.4 \leqslant \mu_I \leqslant 1.0$, we find $\mu_c = 0.394(1)$, $\beta_m = 0.230(9)$ and const $= 1.23(2)$ at a 62% confidence level. This appears inconsistent with mean field scaling for which $\beta_m = \frac{1}{2}$, and closer to the tricritical scaling for which $\beta_m = \frac{1}{4}$. Indeed, good fits to a tricritical scaling form over this range of μ_I and both λ's can be obtained (confidence level 25%).

However, as we have noted in our paper on the quenched theory [4] such fits can be deceptive and can be because the true scaling behavior of these theories is best described by the scaling forms given by effective Lagrangian analyses. When this form of scaling is described in terms of $\mu_I - \mu_c$ rather than the natural scaling variables these forms imply, the true scaling window is very narrow. Outside this window these theories can appear to scale with β_m which is half the true value when analyzed in terms of $\mu_I - \mu_c$. We now introduce the scaling forms (equations of state) suggested by such effective Lagrangians, both of which give mean-field scaling behavior.

The form for the equation of state suggested by the lowest order tree-level analysis of effective Lagrangians of the nonlinear sigma model type [3] is given in terms of α which minimizes the effective potential

$$\mathcal{E} = -a\mu^2 \sin^2(\alpha) - bm\cos(\alpha) - b\lambda\sin(\alpha) \tag{14}$$

in terms of which

$$i\langle \bar{\psi}\gamma_5\tau_2\psi\rangle = b\sin(\alpha) \tag{15}$$

$$\langle \bar{\psi}\psi\rangle = b\cos(\alpha) \tag{16}$$

and

$$j_0^3 = 4a\mu\sin^2(\alpha). \tag{17}$$

b is given in terms of μ_c and a, namely,

$$b = \frac{2}{m}a\mu_c^2. \tag{18}$$

The form for the equation of state which is derived from an effective Lagrangian of the linear sigma model type is obtained by extracting the values of R and α which minimize the effective potential

$$\mathcal{E} = \frac{1}{4}R^4 - \frac{1}{2}aR^2 - \frac{1}{2}b\mu^2\sin^2(\alpha) - cmR\cos(\alpha) - c\lambda R\sin(\alpha) \tag{19}$$

in terms of which

$$i\langle \bar{\psi}\gamma_5\tau_2\psi\rangle = cR\sin(\alpha) \tag{20}$$

$$\langle \bar{\psi}\psi\rangle = cR\cos(\alpha) \tag{21}$$

and

$$j_0^3 = 2b\mu R^2\sin^2(\alpha). \tag{22}$$

c is given in terms of μ_c by

$$c = \frac{b\mu_c^2}{m}\sqrt{a + b\mu_c^2}. \tag{23}$$

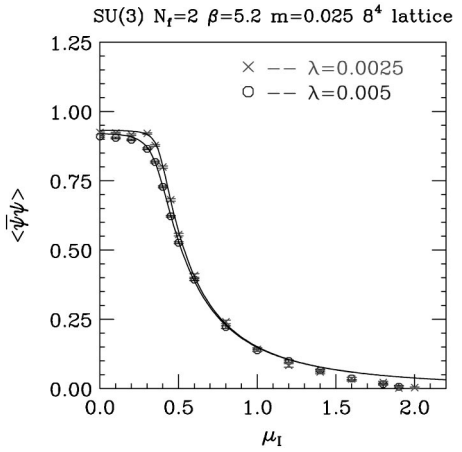

FIG. 2. Chiral condensate as a function of μ_I for $\lambda = 0.0025$ and $\lambda = 0.005$.

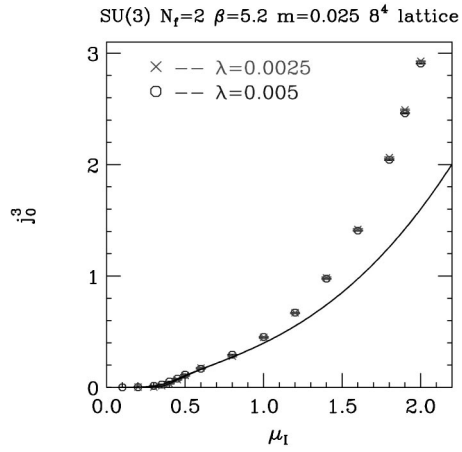

FIG. 3. Isospin (I_3) density as a function of μ_I for $\lambda = 0.0025$ and $\lambda = 0.005$.

Finally, the tricritical scaling form which we use for comparison, and which does not yield mean-field behavior, is expressed in terms of the value of ϕ which minimizes the effective potential (see for example [11])

$$\mathcal{E} = \frac{1}{6}\phi^6 - \frac{1}{3}c\lambda\phi^3 - \frac{1}{2}(\mu_I - \mu_c)\phi^2 - b\lambda\phi \qquad (24)$$

in terms of which

$$i\langle\bar{\psi}\gamma_5\tau_2\psi\rangle = b\phi + \frac{1}{3}c\phi^3 \qquad (25)$$

and

$$j_0 = a\phi^2. \qquad (26)$$

We fit our measurements of the charged pion condensate for $0 \leqslant \mu_I \leqslant 1$ and both λs to the linear sigma model form of Eq. (20). We obtained a fit with $\mu_c = 0.4036(5)$, $a = 0.52(1)$, $m = 0.0253(1)$ with $\chi^2/\mathrm{DOF} = 2.2$ (where DOF stands for degree of freedom). Although worse than the tricritical fit, we note that it allows a reasonable fit for $\mu_I < \mu_c$ in addition to $\mu_I > \mu_c$ which the tricritical fit did not. $\mu_c = 0.426(3)$ for the tricritical fit, which is close to the value expected for the apparent tricritical scaling produced by such sigma model scaling. One of the reasons the tricritical fit gives better results is that it includes a second symmetry breaking interaction, cubic in the order parameter, which rounds off the curve as μ_I approaches 1.0 allowing a better fit to the ''data.'' Such cubic terms could be incorporated in Eq. (19). However, now there is not one such term but several, which is why this possibility was not considered. Finally, as we shall see below, this fit makes good predictions for the chiral condensate and the isospin density.

In Fig. 2 we present the chiral condensate for the same set of simulations. The general characteristics of these graphs are that $\langle\bar{\psi}\psi\rangle$ remains roughly constant for $\mu_I < \mu_c$, after which it drops rapidly, approaching zero at large μ_I. Although this can qualitatively be thought of as the condensate rotating from the chiral to the isospin-breaking direction, it is not a simple rotation, since the magnitude of the total condensate increases up until saturation effects take over. This contrasts with the predictions of lowest order effective Lagrangians of the non-linear sigma model type where it is a simple rotation. However, in the case of 2-color QCD at finite quark-number chemical potential, whose effective Lagrangian is structurally very similar to that for the theory at hand, the effective Lagrangian chiral perturbation theory calculations have been extended to next-to-leading order [12]. Here, although mean field scaling survives, the rotation of the condensate is accompanied by a rescaling. Such behavior is reproduced at tree level by effective Lagrangians of the linear sigma model variety which we use for our fits to the pion condensate. The predictions these fits make for the behavior of the chiral condensate [Eq. (21)], have been superimposed on the measurements of Fig. 2. Except for small departures at small μ_I, which we attribute to the fact that m for the fit differs slightly from the true $m = 0.025$, these predictions are very good until the effects of saturation start to dominate.

Figure 3 presents the isospin (I_3) density as a function of μ_I. While the two condensates are normalized to 4 flavors for comparison with previous ($\mu_I = 0$) simulations, j_0^3 is normalized to 8 flavors, which is the natural normalization for staggered quarks. Qualitatively, we note that j_0^3 is close to zero for $\mu_I < \mu_c$, rises slowly (in comparison with the pion condensate) up to $\mu_I \sim 1$, after which it starts to rise more rapidly reaching its saturation value of 3 (1/2 for each of 3 colors and 2 ''flavors'' per site) due to Fermi statistics at $\mu_I \sim 2$. (In fact measurements made at $\mu_I = 3.0$ give a value consistent with 3.) Saturation is clearly a finite lattice spacing effect and hence requires no further discussion. We also note that there is very little λ dependence. The predictions of Eq. (22) using the parameters of our fit are superimposed on our ''data'' and show good agreement out to $\mu_I \approx 0.8$. Both data and fit are approximately linear in μ_I over this range.

As also noted by Son and Stephanov, measuring j_0^3 as a function of μ_I at $T = 0$ and constant volume (since β is constant) yields the pressure p and energy density ϵ as functions of μ_I, since

$$p = \int_{\mu_c}^{\mu_I} j_0^3 d\mu_I \tag{27}$$

$$\epsilon = \int_0^{j_0^3} \mu_I dj_0^3 \tag{28}$$

for $\mu_I > \mu_c$ and zero for $\mu_I < \mu_c$. In the region where $j_0^3 \approx \text{const} \times (\mu_I - \mu_c)$ these yield

$$p = \frac{1}{2}\text{const} \times (\mu_I - \mu_c)^2 \tag{29}$$

$$\epsilon = \frac{1}{2}\text{const} \times (\mu_I^2 - \mu_c^2) \tag{30}$$

$$\frac{p}{\epsilon} = \frac{\mu_I - \mu_c}{\mu_I + \mu_c}. \tag{31}$$

The last of these equations is a form of the equation of state for this system in the neighborhood of μ_c. Clearly we could extend each of these expressions beyond the scaling region by interpolating the data of Fig. 3 and performing the relevant integrals analytically or numerically.

We performed similar simulations at the same coupling $\beta = 5.2$ and mass $m = 0.05$ at $\lambda = 0.005$ and $\lambda = 0.01$. Here we concentrated on the neighborhood of the phase transition and used more closely spaced (in μ_I) points with somewhat lower statistics. For $\mu_I \gtrsim \mu_c$ we find acceptable fits of the pion condensate to both the non-linear sigma model scaling form and to the tricritical scaling form (34% and 40%, respectively). The fit to the non-linear sigma model effective Lagrangian scaling [Eq. (15)] enables one to extend this to low μ_I. A fit of the data over the complete range over which we have measurements at both λ values—$0.4 \leqslant \mu_I \leqslant 0.7$—yields $\mu_c = 0.569(2)$, $a = 0.0868(9)$ and $m = 0.0534(3)$, with $\chi^2/\text{DOF} = 1.5$ for the non-linear sigma model form. Even though this fit is worse than those restricted to $\mu_I \gtrsim \mu_c$, we feel that the ability to fit $\mu_I < \mu_c$ in addition to $\mu_I > \mu_c$ makes the argument for this form of fit more compelling. Not only do we see qualitative consistency with the smaller mass results, but our measured values of μ_c are consistent with the expectation that $\mu_c(m = 0.05) = \sqrt{2}\mu_c(m = 0.025)$ which would be true if, indeed, $\mu_c = m_\pi$, from PCAC (partial conservation of axial-vector current). This data for the pion condensate with the scaling fits superimposed is plotted in Fig. 4. We note that the fits appear to have validity beyond the range of μ_I over which the fits were performed.

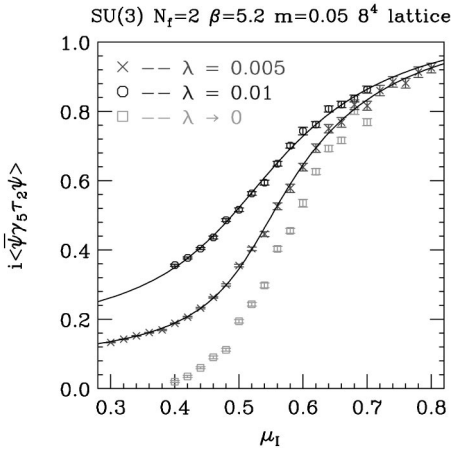

FIG. 4. Pion condensates as functions of μ_I for $\lambda = 0.005$, $\lambda = 0.01$ and a linear extrapolation to $\lambda = 0.0$. The lines are the mean-field fit described in the text.

IV. SIMULATIONS AT FINITE TEMPERATURE

We have performed simulations of QCD at finite μ_I and finite temperature on an $8^3 \times 4$ lattice, with $m = 0.05$. Most of these simulations were performed at $\lambda = 0.005$ and $\lambda = 0.01$, i.e. $\lambda \ll m$, with the objective of obtaining information about the $\lambda = 0$ limit. The goal of these simulations is to map out the region of the (β, μ_I) and hence the (T, μ_I) plane where I_3 is spontaneously broken by a charged pion condensate, and to determine the nature of the phase transitions which demarcate its boundaries.

The first of these simulations was performed at a fixed, large (but well below saturation) value of μ_I. The value chosen was $\mu_I = 0.8$. At β low enough to approximate zero temperature on an $N_t = 4$ lattice, the system is in the phase where I_3 is spontaneously broken by a (large) pion condensate. As β is increased we eventually reach a value $\beta = \beta_c$ at which this condensate evaporates. For $\beta > \beta_c$ we are in the phase where the pion condensate vanishes for $\lambda \to 0$ and I_3 is unbroken. A single λ value, $\lambda = 0.005$, was used for these runs.

Figure 5 shows the β dependence of the pion condensate for these simulations. We see that for $\beta \leqslant 5.2$ the condensate is large. Between $\beta = 5.2$ and $\beta = 5.3$ the condensate drops by an order of magnitude, and is small enough for $\beta \geqslant 5.3$ that we are safe to assume that it would vanish in the $\lambda \to 0$ limit. This drop is so precipitous that we suspect that it is first order, although we really need a larger lattice to confirm this.

We have also measured the thermal Wilson line (Polyakov

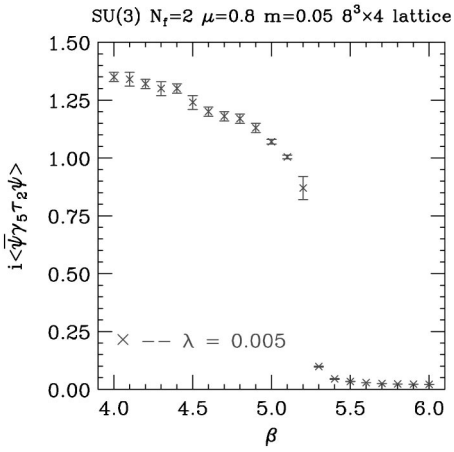

FIG. 5. Pion condensate as a function of β for $m = 0.05$, $\lambda = 0.005$, and $\mu_I = 0.8$ on an $8^3 \times 4$ lattice.

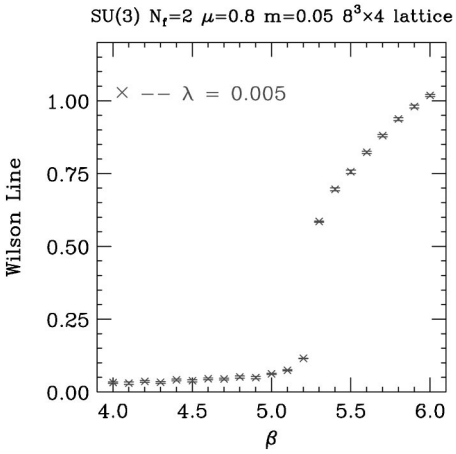

FIG. 6. Wilson line as a function of β for $m=0.05$, $\lambda=0.005$, and $\mu_I=0.8$ on an $8^3\times4$ lattice.

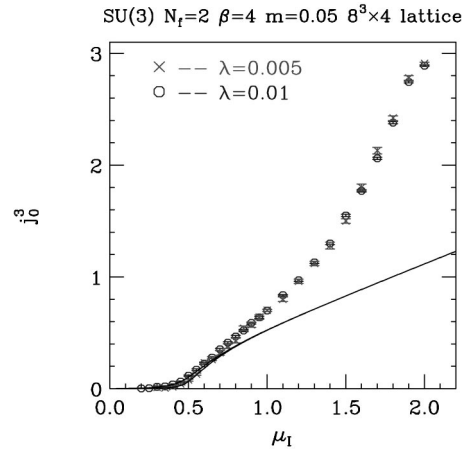

FIG. 8. Isospin (I_3) density as a function of μ_I for $m=0.05$, $\lambda=0.005$ and $\lambda=0.01$ on an $8^3\times4$ lattice at $\beta=4.0$.

loop) during these runs. These measurements are shown in Fig. 6. For $\beta\leqslant5.2$, the Wilson line is small, indicating confinement. For $\beta\geqslant5.3$, the Wilson line becomes large, indicating deconfinement. The jump between $\beta=5.2$ and $\beta=5.3$ is again great enough to suggest a first order transition. This behavior of the Wilson line indicates that this is the temperature-driven deconfinement transition.

We have also run simulations on an $8^3\times4$ lattice with $\beta=4.0$ which gives us the low temperature behavior. We chose $m=0.05$ again and ran at $\lambda=0.005$ and $\lambda=0.01$ for $0.20\leqslant\mu_I\leqslant2.0$ which covers both the transition from the I_3 symmetric phase to the phase where I_3 is spontaneously broken, and the approach to saturation. Our measurements of the pion condensate are shown in Fig. 7. Not surprisingly this graph resembles those we obtained on an 8^4 lattice since at $\beta=4.0$, this lattice is essentially at zero temperature.

We fit the scaling behavior of these measurements to the non-linear sigma model scaling form of Eq. (15) for both λ values and $0.2\leqslant\mu_I\leqslant0.8$. The fit yielded $\mu_c=0.519(1)$, $a=0.1400(4)$ with the quark mass fixed at $m=0.05$ at a confidence level of 41%, which is very good. These fits are shown in Fig. 7. Again an acceptable tricritical fit was possible (confidence level 48%), but only for $0.55\leqslant\mu_I\leqslant0.8$, yielding the expected larger estimate for μ_c.

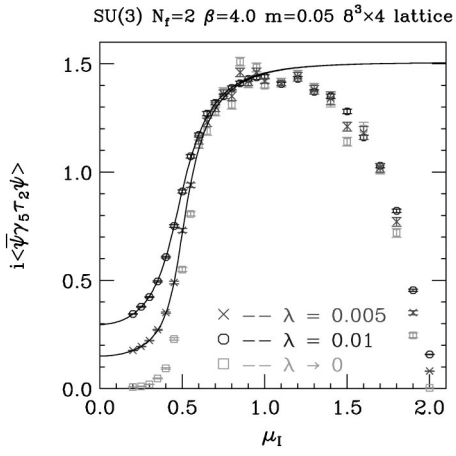

FIG. 7. Pion condensates as functions of μ_I for $\lambda=0.005$, $\lambda=0.01$ and a linear extrapolation to $\lambda=0.0$ on an $8^3\times4$ lattice at $\beta=4.0$. The lines are the mean-field fit described in the text.

In Fig. 8 we present the isospin density from these runs. j_0^3 rises from zero at $\mu_I\sim\mu_c$. Again there is little λ dependence. We have superimposed the form predicted from the fit to pion condensate using Eq. (17) on these plots. These curves are in reasonable agreement with the measured values up to $\mu_I\approx0.7$. This indicates that the scaling window for j_0^3 is slightly less than that for the pion condensate. However, it is clear that the linear or near-linear increase of this quantity with μ_I continues beyond the point where the data and curves diverge. This is born out by the fitting j_0^3 to the form

$$j_0^3=\text{const}\times(\mu_I-\mu_c)^{\beta_I}. \tag{32}$$

Fitting the $\lambda=0.005$ data over the range $0.5\leqslant\mu_I\leqslant1.1$ gives $\mu_c=0.467(13)$, $\beta_I=0.94(6)$ and const$=1.22(3)$ at a confidence level of 18% while fitting the $\lambda=0.01$ data yields $\mu_c=0.382(9)$, $\beta_I=1.09(3)$, const$=1.20(1)$ at a confidence level of 85%. These results are in excellent agreement with the effective Lagrangian prediction $\beta_I=1$. This graph also indicates a crossover to a more rapid increase at $\mu_I\sim1.5$.

Finally we have performed $m=0.05$ simulations on an $8^3\times4$ lattice at $\beta=5.0$, which lies below β_c at high μ_I, while being large enough that the effects of finite temperature should be apparent. Here again we ran with $\lambda=0.005,0.01$. Here we used higher statistics (2000 time units per run) but at fewer μ_I values. Our measurements of the charged pion condensate are presented in Fig. 9. The transition from low to high values of this condensate shows no sign of a first order transition. The linear extrapolation to $\lambda=0$ gives values close to zero at low μ_I, rising rapidly from zero above some $\mu_c\sim0.5$. Here we find good fits of the data for both λ values and $0.2\leqslant\mu_I\leqslant1.0$ to the non-linear sigma model form with $\mu_c=0.5521(5)$, $a=0.1040(4)$, $m=0.0523(1)$ at a confidence level of 31% and to the linear sigma model form with $\mu_c=0.5513(5)$, $a=2.46(1)$, $b=0.0823(4)$, $m=0.0518(1)$ at a confidence level of 48%.

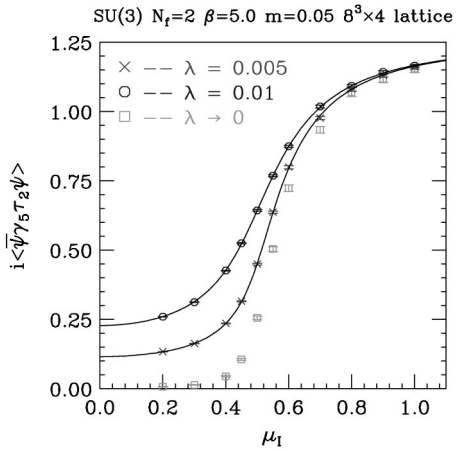

FIG. 9. Pion condensates as functions of μ_I for $\lambda=0.005$, $\lambda=0.01$ and a linear extrapolation to $\lambda=0.0$ on an $8^3\times4$ lattice, at $\beta=5.0$. The lines are the mean-field fit described in the text.

This second fit is included in Fig. 9. A tricritical fit is possible for $0.55\leqslant\mu_I\leqslant0.8$ and has a confidence level of 28%.

Thus the line of phase transitions which bound the region in the (μ_I,T) plane, within which isospin (I_3) is broken spontaneously by a charged pion condensate, is second order for low temperatures and becomes first order at high μ_I. The second order segment of this line appears to have mean-field critical exponents.

V. DISCUSSION AND CONCLUSIONS

We have simulated QCD with 2 quark flavors (u,d) at a finite chemical potential (μ_I) for isospin, I_3. At zero temperature and intermediate coupling $(\beta=6/g^2=5.2)$ we found strong evidence for a second order transition to a phase in which I_3 is spontaneously broken by a charged pion condensate which also breaks parity, at $\mu_I=\mu_c$. The observed behavior is what is predicted by effective Lagrangian methods for μ_I appreciably less than the value at which saturation, a lattice artifact, takes over. These effective Lagrangian analyses predict that $\mu_c=m_\pi$. Since we have not measured m_π on these small lattices, all we have checked is that $\mu_c\propto\sqrt{m}$ for the 2 quark masses which we use $(m=0.025,\ m=0.05)$ and found that this is true within the uncertainties of our measurements. The critical scaling appears to be well described by an equation of state suggested by these effective Lagrangian analyses, which means that the critical point has mean-field critical exponents. However, tricritical behavior cannot be completely excluded. Such behavior was discussed in detail in our paper on the quenched theory [4].

Although we consider our ability to fit to standard mean-field scaling forms to be strong evidence for our claim that the transition is second order with mean field exponents, a word of caution is in order. These measurements were made on a single, relatively small, lattice (8^4). Further simulations on larger lattices will be needed to validate these claims and allow finite size scaling analyses.

We also measured the isospin density (j_0^3) and found that it increases from zero, at or near μ_c. The scaling behavior appears to be linear close to μ_c, as is predicted by effective Lagrangian analyses [3] and well described by the predictions given by the fits to the pion condensate, within the scaling window. For larger μ_I values it starts to increase considerably faster than linear. This is in qualitative agreement with the expectation that I_3 density should increase as μ_I^3 at large μ_I. We have not been able to determine if our observations are consistent with this μ_I^3 increase because of the effects of saturation which cause the isospin density to approach 3 at high μ_I. Here we have indicated how the measurement of j_0^3 enables one to obtain the pressure (p) and the energy density (ϵ) as functions of μ_I, and given explicit expressions for these quantities in the scaling regime.

The chiral condensate remains approximately constant for $\mu_I<\mu_c$. Above μ_c it starts to fall approaching zero for large μ. Again this is in agreement with expectations, and the predictions from the fits to the pion condensate. However, the expectation from the lowest-order effective Lagrangian tree-level analyses, that the chiral condensate simply rotates into the direction of the charged pion condensate, is not true. However, in closely related 2-color QCD at finite quark-number chemical potential, chiral perturbation theory calculations through next-to-leading order show that, while scaling remains mean field, the condensate does not merely rotate, but also rescales [12]. Since the structure of chiral perturbation theory (effective Lagrangians) for the two theories is so similar, we expect a similar result for QCD at finite μ_I.

We have performed simulations at finite temperature (T) in addition to finite μ_I. In particular we have heated the system at fixed $\mu_I=0.8>\mu_c(T=0)$ (in lattice units) by increasing β. On our $N_t=4$ lattice there is some $\beta=\beta_c$ $(5.2\leqslant\beta_c\leqslant5.3)$ at which the charged pion condensate evaporates. This transition appears to be first order. This conclusion, based on the abruptness of the transition, needs validation on larger lattices, where we hope to observe evidence of metastability (as we have for 2-color QCD [8]), which would indicate a first-order rather than a second-order transition. Such first-order behavior was predicted for μ_I large enough by Son and Stephanov [3] who argued that at high μ_I the fermions would effectively decouple, and the phase transition would be that for pure glue, which is known to be first order. We note from our observations that the situation is not quite this simple. The pure glue transition on an $N_t=4$ lattice occurs at $\beta\approx5.7$ [13,14]. Since our observations place β_c somewhat lower than this, and close to the value of the $\mu_I=0$ finite temperature transition, the quarks *are* having an effect. We also note that Son and Stephanov suggest that the first order deconfinement transition at high temperature is distinct from the I_3 symmetry restoring transition. Our evidence is that these 2 transitions are coincident. This means that the second-order segment of the phase boundary can be considered as driven purely by the chemical potential, which makes their argument for $O(2)$ universality less compelling. We note that, in our paper on 2-color QCD at finite μ and T [10], we present an alternative argument for the first-order finite-temperature transition which that theory exhibits for large μ.

In addition, we have simulated our $N_t=4$ system at fixed β, varying μ_I. In particular we have performed simulations at $\beta=4.0$ which is at near-zero temperature, and $\beta=5.0$ where the system is clearly at a finite temperature. Both of these simulations showed evidence for a second order transition. Once again these conclusions are based on simulations on a single small lattice ($8^3\times4$) and simulations on larger lattices will be needed to confirm these observations. Again the scaling was well described by the scaling forms suggested by effective Lagrangian analyses which indicates that they have mean-field critical exponents.

We have noted throughout this paper the similarity between 3-color QCD at finite μ_I and 2-color QCD at finite quark-number chemical potential, μ. The correspondence is seen by identifying $\frac{1}{2}\mu_I$ with μ, the charged pion condensate with the diquark condensate and the isospin density with the quark number density. This similarity is seen both in simulations and in effective Lagrangian analyses. The expected position of the zero temperature transition is the same $\mu_I=m_\pi$ ($\mu=\frac{1}{2}m_\pi$). Its nature—second order with mean-field exponents—is the same as predicted [12] and observed [6,8] for 2-color QCD. In both systems the spontaneous symmetry breaking is in the Goldstone mode (superfluid). At finite temperature the condensate evaporates at a transition which is first order for μ_I (μ) large enough. This line of first-order transitions softens to second order and the line of second-order transitions connects to the zero temperature transition. Thus, we can use 2-color QCD results at finite μ as a guide as to QCD at finite μ_I.

We are extending these simulations to a larger lattice ($12^3\times24$) and weaker coupling where we hope to observe the expected mean-field transition more clearly distinguished from the tricritical alternative and rule out the $O(2)$ alternative. This lattice will also enable us to measure the spectrum of Goldstone and pseudo-Goldstone excitations as functions of μ_I. More extensive spectrum analyses at $\mu_I=0$ will give us a more definitive scale for these phenomena, in addition to a value for m_π with which to compare μ_c. Configurations will be stored so that we can make other spectroscopy measurements at finite μ_I. We will also extend the finite temperature simulations to a $12^3\times6$ lattice since it is difficult to determine the order of the continuum transitions from $8^3\times4$ lattices. In addition we will study the instantons at large μ_I since it is believed that instantons and their interactions have a relatively simple structure at large isospin density, analogous to what has been predicted for large quark-number density [15].

We are also starting lattice QCD simulations, including both a chemical potential μ_I for isospin and a chemical potential μ_s for strangeness. Here effective Lagrangian analyses have indicated that there is a competition between the formation of pion and kaon condensates as μ_I and μ_s are varied independently and that the boundary between the region with a pion condensate and that with a kaon condensate is a line of first-order transitions [16].

Although our simulations have been limited to zero baryon number density, it is interesting to know how much of this analysis is relevant to systems with finite baryon number density and isospin density. If it does have relevance, charged pion condensates could contribute to the equation-of-state of nuclear matter and thus be important in understanding the physics of neutron stars and perhaps large nuclei.

ACKNOWLEDGMENTS

D.K.S. was supported by DOE contract W-31-109-ENG-38. J.B.K. was supported in part by an NSF grant NSF PHY-0102409. J.B.K. wishes to thank D. Toublan for many useful discussions. D.K.S. would like to thank R. Pisarski for emphasizing the importance of extracting pressure and energy density.

[1] Z. Fodor and S.D. Katz, Phys. Lett. B **534**, 87 (2002); J. High Energy Phys. **03**, 014 (2002); S. Choe *et al.*, Phys. Rev. D **65**, 054501 (2002); C.R. Allton *et al.*, hep-lat/0204010; P. de Forcrand and O. Philipsen, hep-lat/0205016; P.R. Crompton, Nucl. Phys. **B619**, 499 (2001); **B626**, 228 (2002).

[2] J.B. Kogut and D.K. Sinclair, Nucl. Phys. B (Proc. Suppl.) **106**, 444 (2002).

[3] D.T. Son and M.A. Stephanov, Phys. Rev. Lett. **86**, 592 (2001); Yad. Fiz. **64**, 899 (2001) [Phys. At. Nucl. **64**, 834 (2001)].

[4] J.B. Kogut and D.K. Sinclair, Phys. Rev. D **66**, 014508 (2002); S. Gupta, hep-lat/0202005.

[5] S. Hands, J.B. Kogut, M.-P. Lombardo, and S.E. Morrison, Nucl. Phys. **B558**, 327 (1999); J.B. Kogut, D.K. Sinclair, S.J. Hands, and S.E. Morrison, Phys. Rev. D **64**, 094505 (2001).

[6] R. Aloisio, V. Azcoiti, G. Di Carlo, A. Galante, and A.F. Grillo, Phys. Lett. B **493**, 189 (2000); Nucl. Phys. **B606**, 322 (2001).

[7] A. Nakamura, Phys. Lett. **149B**, 391 (1984); S. Muroya, A. Nakamura, and C. Nonaka, nucl-th/0111082.

[8] J.B. Kogut, D. Toublan, and D.K. Sinclair, hep-lat/0205019.

[9] J.B. Kogut, M.A. Stephanov, and D. Toublan, Phys. Lett. B **464**, 183 (1999); J.B. Kogut, M.A. Stephanov, D. Toublan, J.J.M. Verbaarschot, and A. Zhitnitsky, Nucl. Phys. **B582**, 477 (2000).

[10] J.B. Kogut, D. Toublan, and D.K. Sinclair, Phys. Lett. B **514**, 77 (2001).

[11] I.D. Lawrie and S. Sarbach, in *Phase Transitions and Critical Phenomena* (Academic Press, London, 1972), Vol. 9.

[12] K. Splittorff, D. Toublan, and J.J.M. Verbaarschot, Nucl. Phys. **B620**, 290 (2002).

[13] F.R. Brown *et al.*, Phys. Rev. Lett. **61**, 2058 (1988).

[14] P. Bacilieri *et al.*, Phys. Rev. Lett. **61**, 1545 (1988).

[15] D.T. Son, M.A. Stephanov, and A.R. Zhitnitsky, Phys. Lett. B **510**, 167 (2001).

[16] J.B. Kogut and D. Toublan, Phys. Rev. D **64**, 034007 (2001).